J Mater Sci (2009) 44:1793–1799
DOI 10.1007/s10853-009-3265-6

Dielectric and pyroelectric studies of Li-modified rare-earth dysprosium-doped barium strontium sodium niobate ceramics

K. Chandramouli · Ramam Koduri

Received: 10 August 2008 / Accepted: 12 January 2009 / Published online: 7 February 2009

Abstract This paper highlights the dielectric, pyroelectric, and resistivity studies of $Ba_{1.45}Sr_{2.4}Dy_{0.1}Li_xNa_{2-x}Nb_{10}O_{30}$ ($x = 0 \leq x \leq 1.0$) tungsten–bronze-structured ceramics. X-ray diffraction studies indicated single orthorhombic (*mm2*) phase supported by tolerance factor and average electronegativity difference. The lattice parameters, unit cell volume, axial ratio, and densities are calculated from XRD studies. The experimental densities obtained are about 95% to that of theoretical values. It is found that the unit cell volume enhanced up to $Li_{0.8}$. The effect of Li modification and Dy doping on ε_{RT}, ε_{T_c}, and T_c in BSNN system are discussed. D.C. resistivity studies indicated the positive temperature coefficient of resistivity (PTCR) response in these compositions.

Introduction

Pyroelectrics are materials that become electrically polarized upon an applied temperature change, include lead barium niobate ($Pb_xBa_{1-x}Nb_2O_6$) and barium strontium niobate ($Ba_{1-x}Sr_xNb_2O_6$). The prominently investigated barium sodium niobate is abbreviated as BNN and also known as "Banana" with tungsten bronze (TB) type structure. The tetragonal tungsten bronze (TTB) materials have been investigated at high temperature ($\sim$1250 °C) [1]. The ferroelectric niobates are widely investigated for their excellent electro-optical, pyro, and piezoelectric applications [2–6]. The development of TTB-type structure, $K_2LnNb_5O_{15}$ (Ln = La, Pr, Nd, Gd, Sm, Tb, Dy, Ho, and Y) by solid state reaction method was investigated [7–10]. Many ferroelectric compounds with the TB-structure such as $Ba_2Na_3RNb_{10}O_{30}$ (R = rare earth ions) [11], $Ba_5LaTi_3Nb_7O_{30}$, $Ba_3La_3Ti_5Nb_5O_{30}$ [12], $Ba_5RTi_3Nb_7O_{30}$ [13], $Ba_4Sm_2Ti_4Ta_6O_{30}$ [14], $Ba_5Li_2Ti_2Nb_8O_{30}$ [15], $(K_{0.50}Na_{0.50})_2(Sr_{0.75}Ba_{0.25})_4Nb_{10}O_{30}$ [16], etc. have extensively been studied. It has been observed that some of the compounds of this family show diffuse phase transition [17]. The structural and electrical properties of Dy-doped barium sodium niobate ceramics were investigated [18]. Pyroelectric properties of rare earth-doped strontium barium niobate ferroelectric ceramics (SBN + yRE$_2$0$_3$, where RE = La, Nd, and Gd) were investigated [19]. BSNN being a lead-free ferroelectric material was chosen in our study owing to the importance of its TB-structured material. To the best of author's knowledge, there is no report on lithium-modified and Dy-doped BSNN ceramics. We report the influence of Li-modified and rare-earth dysprosium-doped $Ba_{1.6}Sr_{2.4}Na_2Nb_{10}O_{30}$ (BSDLNN) ceramic system for dielectric, pyroelectric, and D.C. resistivity studies. The stoichiometric compositions are represented in Table 1.

Experimental methods

Analytical reagent grade $BaCO_3$, $SrCO_3$, Na_2CO_3, Li_2CO_3, Nb_2O_5, and Dy_2O_3 powders were used to prepare BSDLNN

K. Chandramouli
Solid State Physics and Materials Research Laboratory, Department of Physics, Andhra University, Visakhapatnam, India

R. Koduri (✉)
Departmento de Ingenieria de Materials, (DIMAT), Facultad de Ingenieria, Universidad de Concepcion, Concepcion, Chile
e-mail: ramamk@udec.cl

Table 1 Stoichiometric compositions of BSDLNN ceramics

Composition	Formulae
BSNN	$1.6BaCO_3 + 2.4SrCO_3 + Na_2CO_3 + 5Nb_2O_5 \rightarrow Ba_{1.45}Sr_{2.4}Na_2Nb_{10}O_{30} + 5CO_2\uparrow$
BSNN + Li	$1.6BaCO_3 + 2.4SrCO_3 + (x/2)Li_2CO_3 + ([2-x]/2)Na_2CO_3 + 5Nb_2O_5 \rightarrow Ba_{1.45}Sr_{2.4}Li_xNa_{(2-x)}Nb_{10}O_{30} + 5CO_2\uparrow$
BSNN + Dy_y + Li_x	$(1.6-[3/2]y)BaCO_3 + 2.4SrCO_3 + (y/2)Dy_2O_3 + (x/2)Li_2CO_3 + ([2-x]/2)Na_2CO_3 + 5Nb_2O_5 \rightarrow Ba_{1.6-(3/2)y}Sr_{2.4}Dy_yLi_xNa_{(2-x)}Nb_{10}O_{30} + (5-[3/2]y)CO_2\uparrow$
BSNN + $Dy_{0.1}$ + Li_x	$1.45BaCO_3 + 2.4SrCO_3 + 0.05Dy_2O_3 + (x/2)Li_2CO_3 + ([2-x]/2)Na_2CO_3 + 5Nb_2O_5 \rightarrow Ba_{1.45}Sr_{2.4}Dy_{0.1}Li_xNa_{(2-x)}Nb_{10}O_{30} + 4.85CO_2\uparrow$
$x = 0.2$	$1.45BaCO_3 + 2.4SrCO_3 + 0.05Dy_2O_3 + 0.1Li_2CO_3 + 0.9Na_2CO_3 + 5Nb_2O_5 \rightarrow Ba_{1.45}Sr_{2.4}Dy_{0.1}Li_{0.2}Na_{1.8}Nb_{10}O_{30} + 4.85CO_2\uparrow$
$x = 0.4$	$1.45BaCO_3 + 2.4SrCO_3 + 0.05Dy_2O_3 + 0.2Li_2CO_3 + 0.8Na_2CO_3 + 5Nb_2O_5 \rightarrow Ba_{1.45}Sr_{2.4}Dy_{0.1}Li_{0.4}Na_{1.6}Nb_{10}O_{30} + 4.85CO_2\uparrow$
$x = 0.6$	$1.45BaCO_3 + 2.4SrCO_3 + 0.05Dy_2O_3 + 0.3Li_2CO_3 + 0.7Na_2CO_3 + 5Nb_2O_5 \rightarrow Ba_{1.45}Sr_{2.4}Dy_{0.1}Li_{0.6}Na_{1.4}Nb_{10}O_{30} + 4.85CO_2\uparrow$
$x = 0.8$	$1.45BaCO_3 + 2.4SrCO_3 + 0.05Dy_2O_3 + 0.4Li_2CO_3 + 0.6Na_2CO_3 + 5Nb_2O_5 \rightarrow Ba_{1.45}Sr_{2.4}Dy_{0.1}Li_{0.8}Na_{1.2}Nb_{10}O_{30} + 4.85CO_2\uparrow$
$x = 1.0$	$1.45BaCO_3 + 2.4SrCO_3 + 0.05Dy_2O_3 + 0.5Li_2CO_3 + 0.5Na_2CO_3 + 5Nb_2O_5 \rightarrow Ba_{1.45}Sr_{2.4}Dy_{0.1}Li_{1.0}Na_{1.0}Nb_{10}O_{30} + 4.85CO_2\uparrow$

ceramics by solid-state reaction method. The ball-milled powders were calcined at 950 °C for 6 h in a platinum crucible. The fine ground powders were mixed with 5 wt% polyvinyl alcohol binder and compacted (15 mm in diameter and 2 mm of thickness) using steel die and hydraulic press with a uniaxial pressure of 5 tonnes per sq. inch. The binder was burned off at 600 °C and sintered at 1250 °C for 6 h. Powder X-ray diffraction (XRD) studies were carried out by Philips X'pert diffractometer (Cuk_α radiation, $\lambda = 1.5405$ Å). The electroded ceramics were characterized for dielectric properties using digital LCR meter at 1 kHz. Pyroelectric response was measured using Keithley Electrometer model 614 and 8085 microprocessor controlled furnace. A constant voltage of 10 V/cm was applied across the sample to measure D.C. resistivity by a two terminal method.

Results and discussion

X-ray diffraction patterns of BSDLNN ceramics are shown in Fig. 1. BSDLNN ceramics were found to exhibit a single-phase orthorhombic (*mm2*) TB-structure. The lattice parameters, unit cell volume, axial ratio, average particle size, density, tolerance factor (t), and averaged electronegativity (e) of BSDLNN system are given in Table 2. The axial ratio increased up to $Li_{0.8}$. The average particle size was estimated by using Debye-Scherrer model [20]

$$t = (0.89\lambda)/(\beta\cos\theta_B) \quad (1)$$

where λ is the wavelength of target used ($CuK_\alpha = 1.5405$ Å), β is full width at half maximum (FWHM) of the diffraction peak, θ is the corresponding Bragg angle, and t is the diameter of the crystalline. It is evident from Table 2 that Li modification in Dy-doped BSNN system resulted in enhanced lattice parameters in the orthorhombic unit cell. The optimum values of lattice parameters and average particle size are found at $Li_{0.8}$ due to the Li modification and Dy doping in BSNN ceramics influencing the lattice parameters, which in turn has an impact on the orthorhombic unit cell volume. It is quite expected in these systems that the structure or symmetry depends on their processing route and conditions [12]. In our study, the orthorhombic unit cell volume increases along with the axial ratio due to influence of Dy^{3+} substituting Sr^{2+} at A-1 square site, and Li^+ modification supported the unit cell volume expansion until $Li_{0.8}$ which attained saturation and further Li content did not affect the lattice parameters. This could be attributed to ionic radii of the cations modifying BSNN orthorhombic tungsten bronze system. A similar trend was observed with other rare-earth Sm^{3+}

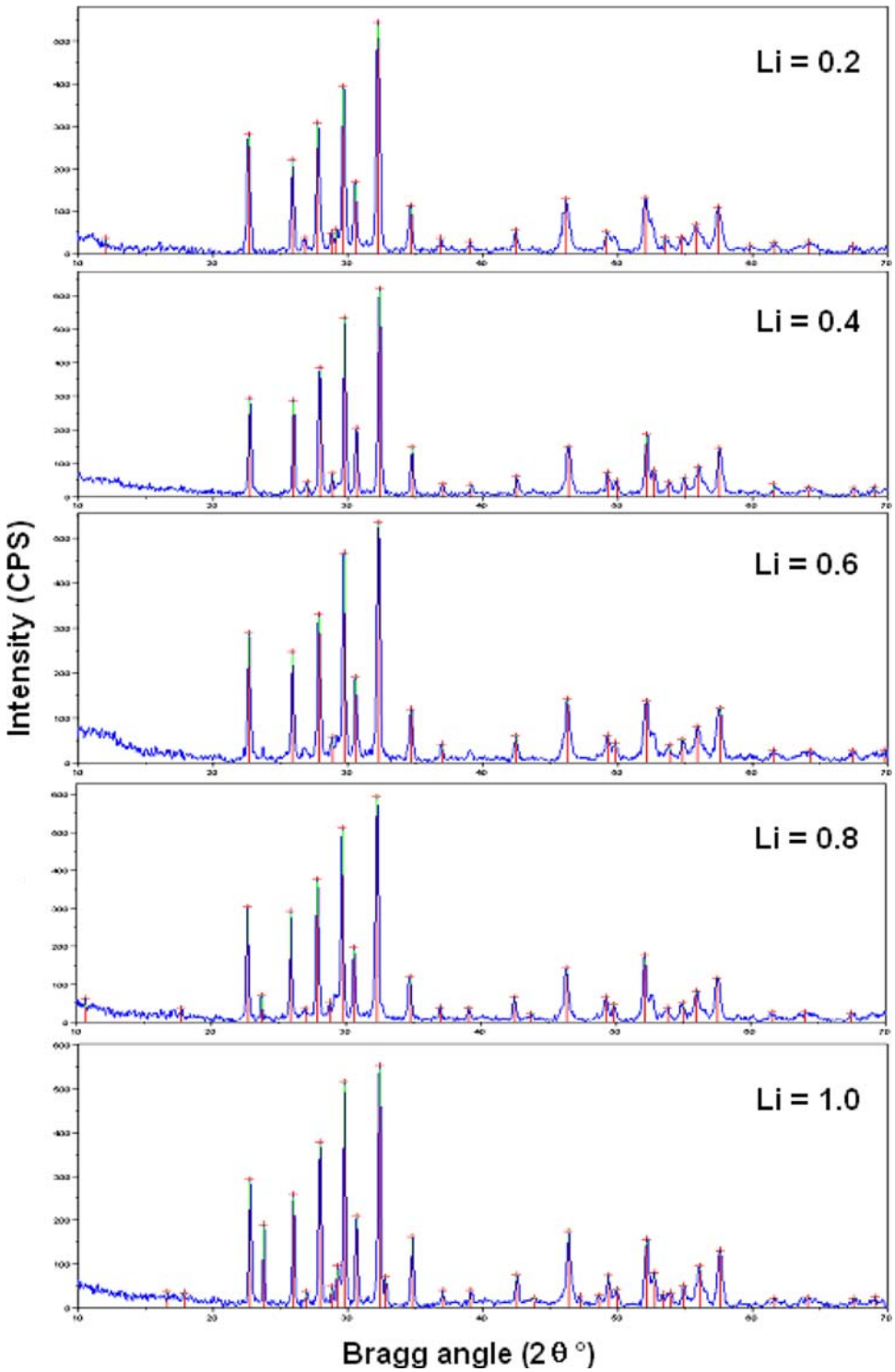

Fig. 1 XRD patterns of BSDLNN ceramics

doped in BSLNN system [21]. The tolerance factor evaluates the degree of the structural stability or distortion that the ionic radius causes [22]. The general formulae of t are shown in Eqs. 2 and 3 for A1 and A2 sites of TB-structure, respectively:

$$t_{A_1} = \frac{r_{A_1} + r_O}{\sqrt{2}(r_B + r_O)} \tag{2}$$

$$t_{A_2} = \frac{r_{A_2} + r_O}{\sqrt{23 - 12\sqrt{3}}(r_B + r_O)} \tag{3}$$

Table 2 Lattice parameters, unit cell volume, axial ratio, particle size, density, t, and e of BSDLNN ceramics

Li	Lattice parameters			Unit cell volume $(Å)^3$	Axial ratio ($\sqrt{10}$ c/a)	Particle size (Å)	Density gm/cm^3	Tolerance factor (t)	Ave. elec. diff. (e)
	a (Å)	b (Å)	c (Å)						
0.2	17.5300	17.5900	3.8700	1193.32	0.6981	4.96	323	0.6417	2.0881
0.4	17.4990	17.7059	3.8703	1199.15	0.6994	4.67	306	0.6412	2.0875
0.6	17.4758	17.5625	3.8722	1188.45	0.7006	4.85	325	0.6406	2.0869
0.8	17.4893	17.6407	3.9294	1212.31	0.7104	4.61	369	0.6400	2.0862
1.0	17.5308	17.5905	3.8705	1193.56	0.6981	4.88	347	0.6394	2.0856

where, r_A, r_B, and r_O are the ionic radii of the A and B site cations, and O^{2-} anions, respectively. The averaged tolerance factor (t) can be denoted in Eq. 4.

$$t = \frac{t_{A_1} + 2t_{A_2}}{3} \tag{4}$$

Alternatively, the averaged electronegativity difference (e) is another important parameter to evaluate the stability of the crystal structure.

$$e = \frac{(\chi_A - \chi_O) + (\chi_B - \chi_O)}{2} \tag{5}$$

where χ_A, χ_B, and χ_O are the individual electronegativities of A and B-site cations, and O^{2-} anions, respectively. The e of BSDLNN ceramics can be written as:

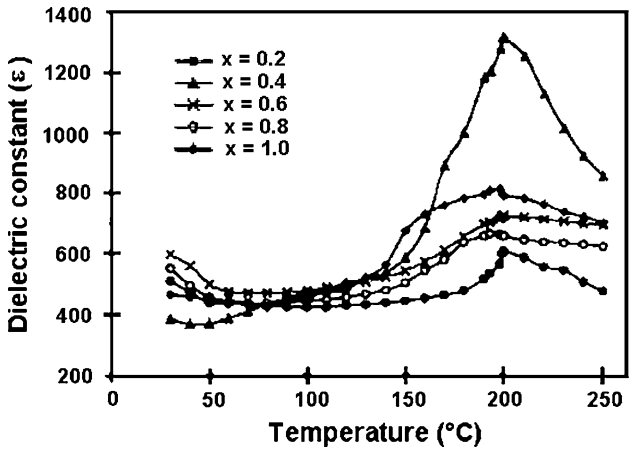

Fig. 2 Dielectric properties of BSDLNN ceramics

$$e = \frac{\{((1.6 - (3/2)y)\chi_{Ba-O} + 2.4\chi_{Sr-O} + y\chi_{Dy-O} + x\chi_{Li-O} + (2-x)\chi_{Na-O} + 10\chi_{Nb-O})\}}{((32-y)/2)} \tag{6}$$

It is evident from Table 2 that there is no distortion in orthorhombic BSDLNN tungsten–bronze structure.

The dielectric properties of BSDLNN ceramics are shown in Fig. 2. It is observed that maximum ε_{RT} is found in $Li_{0.6}$. In our previous investigation, Li modification in pure BSNN system enhanced the ε_{T_c} values up to $Li_{0.4}$ and then decreased with further increase of lithium concentration. The substituted ionic size and their site occupancy play an important role where Na^+ occupies A2-site and Li^+ enters the smaller C sites. The dielectric response in Li-modified BSNN compositions has been observed to be broad [23]. A similar trend in ε_{RT} was reported for $Ba_5MTi_3Ta_7O_{30}$ (M = Ce, Pr, Nd, Sm, Gd, Dy, and Bi) [24]. The ferroelectric nature of Nb-based compounds in a binary system consisting of BNN and BSN together in BSNN system which is further doped with Dy and modified by Li could be the reason for the high ε_{RT}. The T_c continuously decreased which may be due to doping of Dy^{3+} and Li modification in BSLNN ceramics. In the para-electric region, Curie-Weiss law has been obeyed. The curie constant has been calculated and found in the order of 10^5 K indicating that the materials belong to oxygen octahedra ferroelectrics. There is no much change in the dielectric loss, tan δ, with the Li^+ content of $Li_0 = 0.06$ and $Li_1 = 0.05$. The increase in ε_{T_c} was found maximum at $Li_{0.4}$. It is expected that as the ionic radii increase, the unit cell volume eventually increased resulting in enhanced ε_{RT}. Substitution of rare-earth Dy into BSLNN yielded high ε_{RT}, ε_{T_c} and low T_c and tan δ. This could be attributed to the combined effect of alkali Li modification and rare-earth Dy doping in BSNN system.

Figure 3 indicates the pyroelectric response of BSDLNN ceramics. The pyroelectric coefficient has been calculated from the general formula:

$$P = \frac{dp}{dt} \tag{7}$$

where dp and dt are change in polarization and temperature, respectively. The quality of the pyroelectric

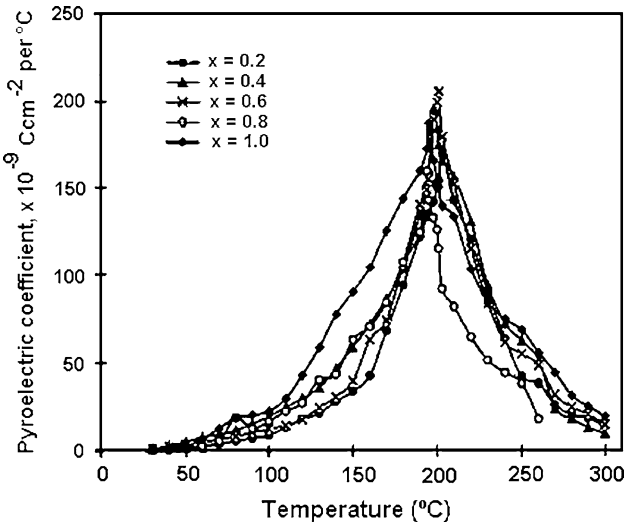

Fig. 3 Pyroelectric properties of BSDLNN ceramics

materials can be evaluated through different figure of merits:

$$\text{Voltage responsitivity, } \mathrm{FM_{RV}} = \frac{P}{\rho C_{\mathrm{p}} K} \tag{8}$$

$$\text{Normalized detectivity, } \mathrm{FM_{RN}} = \frac{P}{\rho C_{\mathrm{p}} \sqrt{K}} \tag{9}$$

$$\text{Current responsitivity, } \mathrm{FM_{RI}} = \frac{P}{\rho C_{\mathrm{p}}} \tag{10}$$

where C_p is the specific heat. The pyroelectric coefficients have increased up to $Li_{0.6}$ which followed the trend of dielectric response. It is observed that the P_{T_c} trend coincides with T_c. The highest value of $P_{RT} = 1.50 \times 10^{-9}$ C/cm^2 °C and $P_{max} = 2.05 \times 10^{-7}$ C/cm^2 °C, respectively, are obtained in $Li_{0.6}$. A similar behavior has been observed in Pr/Nd-BSNN material [25]. The values of figure of merit FM_{RV}, FM_{RN}, and FM_{RI} were calculated and found in the order of 10^{-14} CM/J, 10^{-12} CM/J, and 10^{-11} CM/J, respectively, which have been represented in Table 3. These values are one order less when compared with single crystal of BSKNN [26], and Pr/Nd-BSNN [25]. This behavior was observed due to Dy doping and Li modification in BSNN system which influenced the ceramic polarization probably substituting isovalent Ba^{2+} and Sr^{2+} ions, generating excess positive charges, which are electronically compensated by cationic vacancies. On the contrary, La- and Nd-doped SBN showed a decreasing polarization trend and three distinct anomalies due to the off-valence doping in the tetragonal tungsten bronze structure which can reduce the tetragonality factor (c/a) and, consequently, T_m [27].

The D.C. resistivity study is calculated using the following formula:

Table 3 Dielectric, pyroelectric, and D.C. resistivity studies of BSDLNN ceramics

Li	$P_{RT} \times 10^{-9}$ C/cm^2 °C	$P_{max} \times 10^{-7}$ C/cm^2 °C	P_{T_c}(°C)	ε_{RT}	ε_{T_c}	T_c (°C)	Curie constant C × 10^5 K	$FM_{RV} \times 10^{-14}$ CM/J	$FM_{RN} \times 10^{-12}$ CM/J	$FM_{RI} \times 10^{-11}$ CM/J	$\rho_{RT} \times 10^7$ Ω cm	$\rho_{max} \times 10^{10}$ Ω cm	Activation energy (eV)	
													$+E_a$	$-E_a$
0.2	0.62	1.68	203	509	604	200	5.51	0.74	0.16	0.37	1.4	0.93	0.2124	0.1924
0.4	1.43	1.95	198	384	1311	199	9.09	2.41	0.45	0.92	0.7	1.14	0.2151	0.2045
0.6	1.50	2.05	201	596	721	200	1.90	1.57	0.38	0.93	1.8	0.83	0.2352	0.2117
0.8	0.98	1.59	195	550	660	193	2.50	1.17	0.27	0.64	1.9	1.02	0.2204	0.2097
1.0	0.83	1.86	195	465	810	198	4.06	1.10	0.23	0.51	1.2	0.98	0.2312	0.2125

$$\rho = RA/l\,\Omega\,\mathrm{cm} \tag{11}$$

where R is the resistance, $A = \pi r^2$ = surface area, r is radius, l is the thickness, and ρ is the resistivity of the sample. The activation energies of the samples were estimated from the variation of resistivity with temperature and calculated using the following relation:

$$2.3026\,\frac{\mathrm{d}y}{\mathrm{d}x} = \frac{E_a}{K} \tag{12}$$

(or)

$$E_a = 2.3026 \times K \times \frac{\mathrm{d}y}{\mathrm{d}x} \tag{13}$$

where E_a is the activation energy, K = Boltzmann constant (8.61×10^{-5} eV), and $\mathrm{d}y/\mathrm{d}x$ is the slope of the line between log ρ and $1/T$.

Figure 4 indicates D.C. resistivity of BSDLNN ceramics. The resistivity in these compositions increased with temperature and Li addition, and at a certain temperature (P_{T_c}), resistivity decreased indicating the positive temperature coefficient of resistivity (PTCR) behavior. It is interesting to note that a positive temperature coefficient of resistance (PTC) behavior has been observed in all the compositions. A similar trend was observed in Pr-BLN [25]. The temperatures at which the resistivity begins to drop off in the compositions match with the values of T_c from the dielectric response and maximum pyroelectric coefficient corresponding temperatures from the pyroelectric studies. A similar trend was observed in Pr-BLN [28]. In all the compositions of BSDLNN, the values of ρ_{T_c} are much below the values of T_c. A similar trend has been reported in rare-earth ion-modified barium copper niobate and barium copper tantalite [29] and Pr-BLN [28]. It is observed that the resistivity values change in the order from 0.7×10^7 Ω cm to 1.14×10^{10} Ω cm and have been given in Table 3. The maximum resistivity, ρ_{max} (1.14×10^{10} Ω cm) is found in $Li_{0.4}$. The ρ_{max} is in the order of 10^{10} Ω cm which is three orders larger when compared with the ρ_{RT}. The activation energies in both positive and negative regions of temperature versus resistivity have been calculated and given in Table 3. The increase in ρ_{max} and activation energy may be due to the presence of Dy and Li in BSNN. Thus, these materials indicate that they are suitable for pyroelectric or PTCR applications.

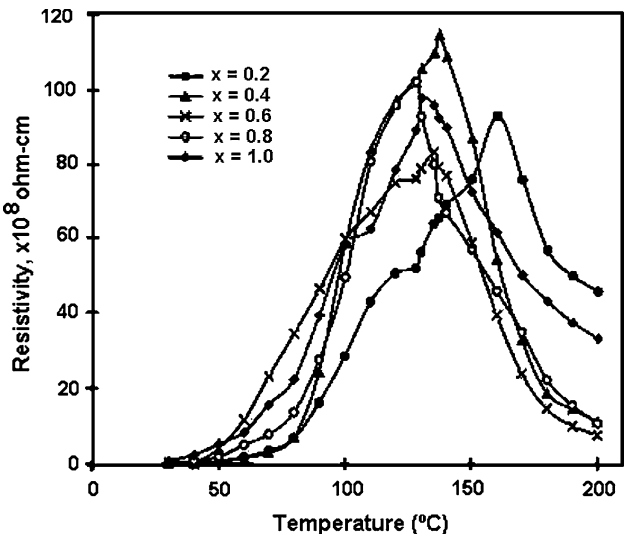

Fig. 4 D.C. resistivity of BSDLNN ceramics

Conclusions

In summary, Li-modified Dy-doped BSNN ceramics have exhibited single phase orthorhombic tungsten bronze structure supported by tolerance factor and average electronegativity difference. The maximum values of lattice parameters are found in $Li_{0.8}$. The optimum dielectric response is found in $Li_{0.6}$. The highest P_{RT} and P_{max} are obtained in $Li_{0.6}$. The values of figure of merit, FM_{RV}, FM_{RN}, and FM_{RI} are calculated and found in the order of 10^{-14} CM/J, 10^{-12} CM/J, and 10^{-11} CM/J, respectively. The nature of variation in resistivity shows the positive temperature coefficient of resistance (PTCR) behavior in BSDLNN ceramics. The maximum resistivity, ρ_{max} (1.14×10^{10} Ω cm) is found in $Li_{0.4}$. Thus, it is concluded that high ε_{RT}, ε_{T_c}, FM_{RV}, FM_{RN}, and FM_{RI} with low T_c and tan δ may be useful for pyroelectric or PTCR applications.

Acknowledgements The authors would like to thank Andhra University, Visakhapatnam, India, and University of Concepcion, Chile. The authors acknowledge Ms. C. N. Devi, Mr. Ranganathan, and Mr. Krishnamurthy for their valuable technical support extended during this work.

References

1. Neurgaonkar RR, Nelson JG, Oliver JR (1990) Mater Res Bull 25:959
2. Hirano H, Takei H, Koide S (1969) J Appl Phys 8:172
3. Lenzo PV, Spencer EG, Ballman AA (1969) Appl Phys Lett 11:972
4. Glass M (1969) J Phys 40:4699
5. Yamanchi H (1978) Appl Phys Lett 32:599
6. Nakano J, Yamada T (1975) J Appl Phys 46:2361
7. Brenden I, Kennedy J, Hunter BA (1999) J Mater Res Bull 34:1263
8. Mergen A, Lee WE (1997) J Mater Res Bull 32:175
9. El Haimouti A, Zambon D, El-Ghozzi M, Avignant D, Leroux D, El Aatmani M, Daoud M (2003) Mater Res Bull 38:1423
10. Kahoul A, Nkeng P, Hammouche A, Nâamoune F, Poillert G (2001) J Solid State Chem 161:397
11. Singh S, Sati R, Choudhary RNP (1992) J Mater Sci Lett 11:788
12. Zheng XH, Chen XM (2003) Solid State Commun 125:449

13. Panigrahi A, Singh NK, Choudhary RNP (1999) J Mater Sci Lett 18:1579
14. Li J, Chen XM, Wu YJ (2002) J Eur Ceram Soc 22:87
15. Dong M, Reau JM, Ravez J (1996) Solid State Ionics 91:183
16. Bu S, Chun D, Park G (1997) Jpn J Appl Phys 36:4351
17. Lines E, Glass AM (1977) Principles and applications of ferroelectrics and related materials. Clarendon, Oxford
18. Subba Rao PSV, Sambasiva Rao K (1990) Ferroelectrics 102(1):183
19. Santos A, Garcia D, Eiras JA (2001) Ferroelectrics 257:105
20. Scheerer's D, Gottin P (1918) Nachricht 2:98
21. Chandramouli K, Viswarupachary P, Ramam K (2008) J Mater Sci Mater Electron. doi:10.1007/s10854-008-9818-7
22. Chandramouli K, Srinivas Reddy G, Ramam K (2008) Scr Mater 59(2):235
23. Chandramouli K, Viswarupachary P, Naidu MS (2005) Ferroelectrics 325:3
24. Bijumon PV, Kohli V, Prakash Om, Varma MR, Sebastian MT (2004) Mater Sci Eng B 113:13
25. Sambasiva Rao K, Prasad TNVKV, Vallishnath N, Lee JH, Cho S-H (2003) Ferroelectr Lett 30:25
26. Neurgaonkar RR, Cory WK, Oliver JR, Clark WWIII, Wood GL, Miller MJ, Sharp EJ (1987) J Cryst Growth 84:629
27. Garcia D (1995) PhD Thesis, University of Siio Paulo, SBo Carlos—SP, Brazil
28. Sambasiva Rao K, Koteswara Rao K, Viswarupachary P (1991) Proc Natl Acad Sci India 69:I
29. Sambasiva Rao K, Jagga Rao PS, Rama Rao K, Prasada Rao AV, Robin AI, Tandon RP (1993) Indian J Pure Appl Phys 31:43